ChemComm

COMMUNICATION

View Article Online
View Journal | View Issue

Cite this: *Chem. Commun.*, 2019, **55**, 13144

Received 4th September 2019,
Accepted 7th October 2019

DOI: 10.1039/c9cc06904f

rsc.li/chemcomm

Visible light induced redox neutral fragmentation of 1,2-diol derivatives†

Kang Chen,‡ Johanna Schwarz,‡ Tobias A. Karl, Anamitra Chatterjee and Burkhard König*

A homogeneous, redox-neutral photo fragmentation of diol derivatives was developed. Under photo/hydrogen atom transfer (HAT) dual catalysis, diol derivatives such as lignin model compounds and diol monoesters undergo selective β C(sp^3)–O bond cleavage to afford ketones, phenols and acids effectively.

Diol and polyol derivatives are the fundamental structural units of lignin, which is an important renewable non-fossil organic carbon source.[1] The selective C(sp^3)–O bond cleavage of diol or polyol derivatives could offer a sustainable approach to gain valuable oxygen-containing feedstock chemicals from lignin biomass.[2] Photochemical C–O bond cleavage processes may proceed under mild conditions,[3] opening perspectives of solar driven lignin valorization. The selective deoxygenation of lignin β-O-4 model compounds, a type of aromatic backbone diol derivative, has been realized by using Ir photocatalysts, organic copolymers or semi-conductors under UV-Vis irradiation (Scheme 1A).[4–6] These step-wise deoxygenation reactions involved oxidation and reduction processes to achieve an overall redox-neutral transformation. However, the use of stoichiometric amounts of external oxidants and reductants were still necessary.

The hydroxyl groups in diols are already a reductive hydrogen source. Thus, the catalytic hydrogen transfer[7] from the hydroxyl group to the β C(sp^3)–O bond would be an ideal strategy for the redox-neutral deoxygenation in one single step without external reductants. Very recently, heterogeneous photocatalysts such as $ZnIn_2S_4$ and CdS quantum dots were applied in the redox-neutral degradation of lignin β-O-4 model compounds in absence of stoichiometric external reductants (Scheme 1B).[8] Herein, we report the homogeneous, redox neutral photocatalytic fragmentation of diols using two different photo/HAT dual catalytic systems (Scheme 1C).

We began the optimization of the reaction conditions with diol derivative **1a**. After screening of metal photocatalysts, HAT catalysts, and solvents (see ESI,† for detailed information), we discovered that the combination of $[Ir(ppy)_2dtbpy]PF_6$ and methyl 2-mercaptoacetate as co-catalyst in DMA solution facilitates the cleavage of **1a** into ketone (**2a**) and phenol (**3a**) in 91% and 81% yield, respectively (Table 1, entry 1). Sodium dibutylphosphate was the crucial base for this reaction, because it shows good solubility in organic solvents and accelerates the generation of thiyl radicals (S–H BDE = 87 kcal mol^{-1})[9] as HAT agents.[10] Moreover, this base is also a good hydrogen bond acceptor, which could effectively activate the α C–H bond of the hydroxyl group to promote the following H-atom abstraction (α C–H bond BDE = 86 kcal mol^{-1}).[11,12] Notably, the use of stoichiometric phosphate was necessary to achieve high yields of products (Table 1, entries 1 and 2). Other insoluble inorganic bases (K_2CO_3, Na_2HPO_4 *etc.*) or the organic base 2,4,6-collidine gave significantly lower yields (Table S2, ESI†). Control experiments

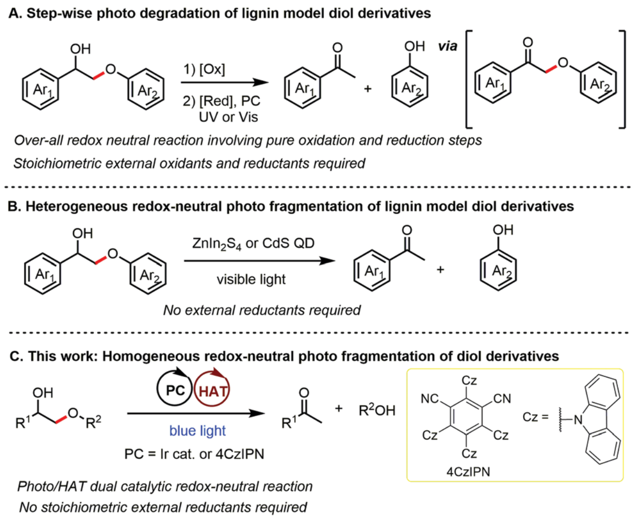

Scheme 1 Photo fragmentation of diol derivatives.

Faculty of Chemistry and Pharmacy, University of Regensburg, 93040 Regensburg, Germany. E-mail: burkhard.koenig@ur.de

† Electronic supplementary information (ESI) available. See DOI: 10.1039/c9cc06904f

‡ These authors contributed equally to this work.

Table 1 Optimization of redox-neutral fragmentation of **1a**

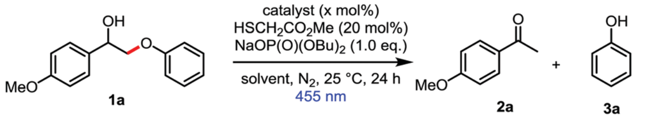

Entry[a]	Catalyst (x mol%)	Solvent	Ketone	Phenol
1	$[Ir(ppy)_2dtbpy]PF_6$ (1)	DMA	91% (86%)[b]	81% (71%)[b]
2[c]	$[Ir(ppy)_2dtbpy]PF_6$ (1)	DMA	40%	30%
3[d]	$[Ir(ppy)_2dtbpy]PF_6$ (1)	DMA	16%	Trace
4	Eosin Y (5)	DMA	n.d.	n.d.
5	Perylene (5)	DMA	n.d.	n.d.
6	4CzIPN (5)	DMA	26%	26%
7[d]	4CzIPN (5)	DMA	59%	48%
8[d,e]	4CzIPN (10)	DMA	72%	44%
9[d,e]	4CzIPN (10)	DMSO	73%	54%
10[d,e]	4CzIPN (8)	DMSO	76%	58%
11[d,e]	4CzIPN (4)	DMSO	82%	57%
12[c,d,e]	4CzIPN (4)	DMSO	80% (79%)[b]	57% (63%)[b]

[a] 0.1 mmol scale reaction; yields determined by GC analysis with an internal standard. [b] Isolated yield. [c] 50 mol% $NaOP(O)(OBu)_2$. [d] Under air atmosphere. [e] 40 mol% $HSCH_2CO_2Me$.

Table 2 Photo fragmentation of lignin β-O-4 model diol derivatives

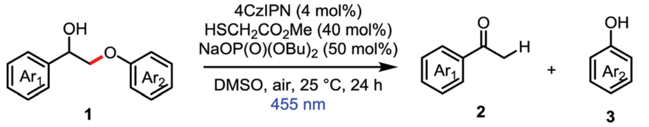

Entry[a]	Substrate	Ketone	Phenol
1	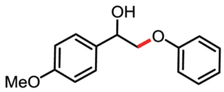 **1a**	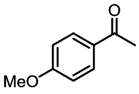 **2a** (79%) (86%)[b]	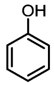 **3a** (63%) (71%)[b]
2	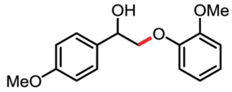 **1b**	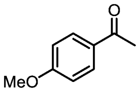 **2a** (69%)	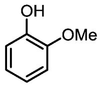 **3b** (51%)
3	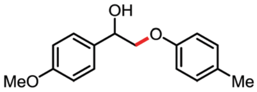 **1c**	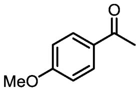 **2a** (90%)	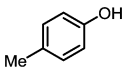 **3c** (61%)
4	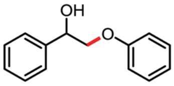 **1d**	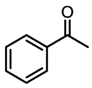 **2b** (69%)	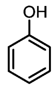 **3a** (50%)
5	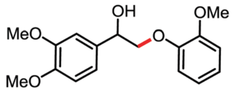 **1e**	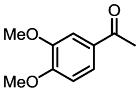 **2c** (75%)	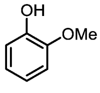 **3b** (61%)
6	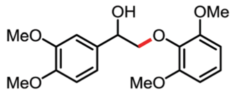 **1f**	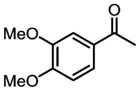 **2c** (83%)	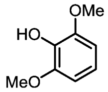 **3d** (76%)
7	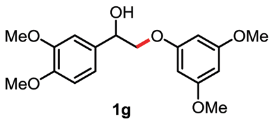 **1g**	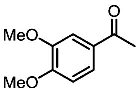 **2c** (quant.)	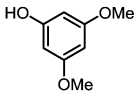 **3e** (84%)
8	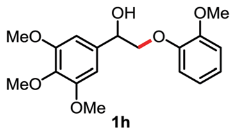 **1h**	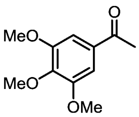 **2d** (68%)	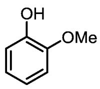 **3b** (33%)
9	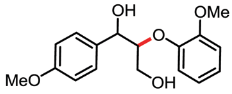 **1i**	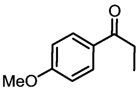 **2e** (trace) (trace)[bc]	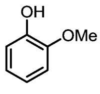 **3b** (20%)[c] (n.d.)[bc]

[a] Reactions were carried out in 0.1 mmol scale, isolated yields are reported. [b] 1 mol% of $[Ir(ppy)_2(dtbpy)]PF_6$, 20 mol% of $HSCH_2CO_2Me$ and 1.0 equiv. of $NaOP(O)(OBu)_2$ in 2.0 mL DMA (0.2 mmol scale) under N_2 atmosphere. [c] Determined by GC analysis.

indicated that Ir catalyst, thiol catalyst, base, light irradiation (Table S5, ESI†) and inert atmosphere (Table 1, entry 3) were all essential for this transformation.

Although the Ir catalyst performs quite well in this reaction, the high price and toxicity of iridium limits its application. We therefore tested different redox active organic dyes[13,14] to explore the possibility of a transition-metal free catalytic system for this transformation. Eosin Y and perylene did not catalyze the C(sp^3)–O bond cleavage (Table 1, entries 4 and 5) while with 5 mol% 4CzIPN as catalyst, the generation of aryl ketone and phenol was observed, albeit in low yields (Table 1, entry 6). To our surprise, the 4CzIPN catalyzed reaction performed even better under air atmosphere (Table 1, entry 7). We could further improve the reaction efficiency by tuning the loading of 4CzIPN and thiol, as well as by using DMSO, instead of DMA (Table 1, entries 8–11). Additionally, the yields of both products remained almost the same even when the amount of $NaOP(O)(OBu)_2$ was decreased to 0.5 equiv. (Table 1, entry 12). Compared with Ir catalysis, the 4CzIPN catalyst system exhibits similar reaction efficiency under more robust conditions (Table 1, entries 1 and 12). Thus, we chose 4CzIPN catalysis for substrate scope investigation.

To probe the generality of this methodology, various lignin β-O-4 model compounds were investigated under the optimized conditions (Table 2). The electronic properties of both aromatic rings (Ar^1 and Ar^2) influence the reactivity of substrates (**1b–d**). Generally, more electron-poor Ar^1 (**1d**) and more electron-rich Ar^2 (**1b**) decreased the conversion of starting material so that comparatively lower product yields were obtained. The coniferyl-derived substrates (**1e–g**) convert smoothly, affording good to excellent yields of the corresponding fragmentation products. However, the sinapyl-derived substrate **1h** was not compatible with the aerobic conditions and reacted less efficient. The branched β-O-4 model compound **1i** did not react well with 4CzIPN or the Ir catalysis. Traces of deoxygenated ketone and not more than 20% phenol were detected. Increased steric hindrance of **1i** inhibiting the benzylic C–H abstraction by thiyl radicals may be a reason for the observation.

Furthermore, we investigated the influence of different leaving groups (Table 3). Similar to the diol mono-phenoxyethers, mono-acetates of diols bearing different substituents underwent selective β C(sp^3)–O bond cleavage to generate aryl ketones and the

Table 3 Photo fragmentation of diol derivatives with various backbones and leaving groups

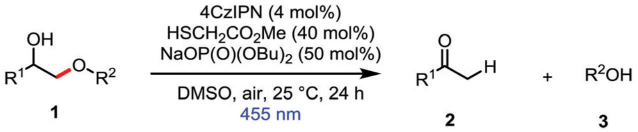

Entry[a]	Substrate	Products	
1–4	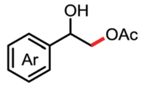 Ar = 4-MeOC$_6$H$_4$, **1j** Ar = C$_6$H$_5$, **1k** Ar = 4-ClC$_6$H$_4$, **1l** Ar = 4-FC$_6$H$_4$, **1m**	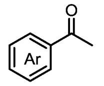 **2a** (70%) **2b** (74%) **2f** (61%) **2g** (75%)	+ AcOH Not Isolated
5	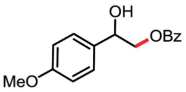 **1n**	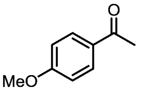 **2a** (73%)	+ 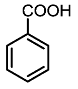 **3f** (70%)
6	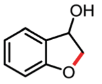 **1o**	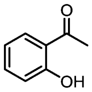 **2h** (45%)	
7[b]	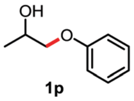 **1p**	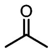 Not Measured	+ 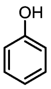 **3a** (72%)

[a] Reactions were carried out in 0.1 mmol scale, isolated yields are reported. [b] 2 mol% of [Ir(ppy)$_2$(dtbpy)]PF$_6$, 40 mol% of HSCH$_2$CO$_2$Me and 1.0 equiv. of NaOP(O)(OBu)$_2$ in 1.0 mL DMA (0.1 mmol scale) under N$_2$ atmosphere for 72 h. Yield determined by GC analysis with an internal standard.

volatile AcOH (**1j–m**). Halogen atoms such as F (**1m**) and Cl (**1l**) are tolerated. Moreover, we could isolate both aryl ketone and benzoic acid in good yields from the reaction of mono-benzoate (**1n**). An intramolecular fragmentation occurred with dihydrobenzofuran derivative **1o** to form the ring-open product 2-hydroxyacetophenone **2h** in moderate yield.

Finally, we also explored the conversion of aliphatic diol derivatives with the photo/HAT dual catalysis strategy. Unfortunately, the 4CzIPN system was not able to catalyze the fragmentation of **1p** under aerobic conditions. The Ir catalyst under inert atmosphere gave the desired phenol product, but higher Ir and thiol catalyst loadings and a longer reaction time were required (Table 3, entry 7). Due to the higher BDE of the aliphatic alcohol α C–H bond (BDE = 92 kcal mol^{-1}, *vs.* benzylic alcohol α C–H BDE = 86 kcal mol^{-1}),[11] cleavage of the α C–H bond of the aliphatic alcohol is more difficult with the thiyl radical.

We also explored the reactivity of free diol and full-protected diester. In case of diol **4**, the ketone product **2a** was detected only in a very low yield (Scheme 2, eqn (1)). Furthermore, the diol diacetate **5** remained untouched under the standard conditions (Scheme 2, eqn (2)). These results suggest that both unprotected hydroxyl group and the adjacent leaving group are crucial for the desired β C(sp^3)–O bond cleavage.

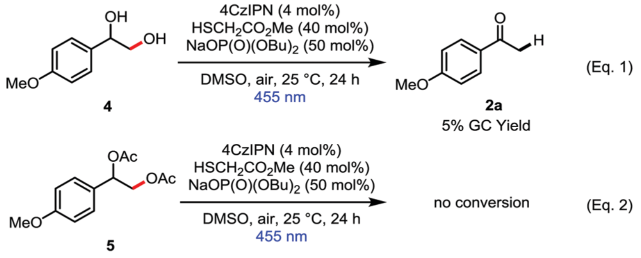

Scheme 2 Control experiments with unprotected and full-protected diol derivatives.

According to quenching experiments (see Fig. S3–S6 in the ESI†), we assume the excited photocatalyst 4CzIPN ($E_{(\mathrm{PC}^{*}/\mathrm{PC}^{\bullet-})}$ = +1.43 V *vs.* SCE)[15] is reductively quenched in the presence of thiol (E_{ox} = +0.85 V *vs.* SCE)[10a] and phosphate. Then the generated thiyl radical abstracts the α H-atom of benzylic alcohol **1** to give a benzylic ketyl radical **A**, which is further oxidized to the corresponding ketone **B**. The generation of ketone **B** could be proven by GC analysis of the crude reaction mixture after four hours of irradiation (see Fig. S7 in the ESI†). A SET reduction of ketone **B** by the reduced photocatalyst results in ketyl radical anion **C**.[16] The intermediate **C** is not stable so that a following β C(sp^3)–O bond cleavage takes place to form the carbonyl radical **D** and the anion of leaving group **E**,[3e,4,8] which are further converted to the final fragmentation products (Scheme 3).

In summary, we have developed a redox neutral fragmentation of diol derivatives *via* photo/HAT dual catalysis without the use of stoichiometric external reductants. Both 4CzIPN and Ir photocatalysts facilitate the fragmentation of diol derivatives such as lignin β-O-4 model compounds and diol monoesters. Mechanistic studies suggest that the substrates are transformed to the corresponding ketones *via* HAT and oxidation. Subsequently, the photo reduction of the ketone generates the ketyl radical anion and induces the β C(sp^3)–O bond cleavage to afford the desired products. The photocatalytic C–O bond cleavage strategy may find application in the valorization of biomass molecules.

This work was supported by the German Science Foundation (DFG) (GRK 1626, Chemical Photocatalysis; KO 1537/18-1).

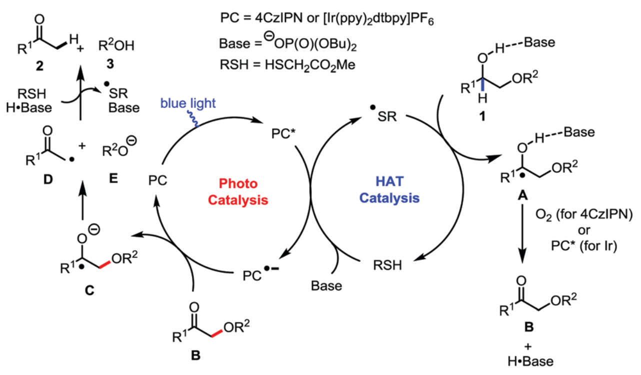

Scheme 3 Proposed mechanism for the photo fragmentation of diol derivatives.

JS and TK thank the Deutsche Bundesstiftung Umwelt (DBU) for a graduate scholarship. KC thanks the Alexander von Humboldt Foundation for a postdoctoral fellowship. We also thank Dr R. Vasold and Ms R. Hoheisel for analytic support.

Conflicts of interest

There are no conflicts to declare.

Notes and references

1 (*a*) J. Zakzeski, P. C. A. Bruijnincx, A. L. Jongerius and B. M. Weckhuysen, *Chem. Rev.*, 2010, **110**, 3552; (*b*) C. O. Tuck, E. Pérez, I. T. Horváth, R. A. Sheldon and M. Poliackoff, *Science*, 2012, **337**, 695; (*c*) A. J. Ragauskas, G. T. Beckham, M. J. Biddy, R. Chandra, F. Chen, M. F. Davis, B. H. Davison, R. A. Dixon, P. Gilna, M. Keller, P. Langan, A. K. Naskar, J. N. Saddler, T. J. Tschaplinski, G. A. Tuskan and C. E. Wyman, *Science*, 2014, **344**, 1246843; (*d*) M. V. Galkin and J. S. Samec, *ChemSusChem*, 2016, **9**, 1544.

2 For selected examples of C(sp^3)–O bond cleavage of lignin system, see: (*a*) N. Yan, C. Zhao, P. J. Dyson, C. Wang, L.-T. Liu and Y. Kou, *ChemSusChem*, 2008, **1**, 626; (*b*) J. M. Nichols, L. M. Bishop, R. G. Bergman and J. A. Ellman, *J. Am. Chem. Soc.*, 2010, **132**, 12554; (*c*) S. Son and F. D. Toste, *Angew. Chem., Int. Ed.*, 2010, **49**, 3791; (*d*) A. G. Sergeev and J. F. Hartwig, *Science*, 2011, **332**, 439; (*e*) T. Kleine, J. Buendia and C. Bolm, *Green Chem.*, 2013, **15**, 160; (*f*) M. V. Galkin, S. Sawadjoon, V. Rohde, M. Dawange and J. S. M. Samec, *ChemCatChem*, 2014, **6**, 179; (*g*) A. Rahimi, A. Ulbrich, J. J. Coon and S. S. Stahl, *Nature*, 2014, **515**, 249; (*h*) C. S. Lancefield, O. S. Ojo, F. Tran and N. J. Westwood, *Angew. Chem., Int. Ed.*, 2015, **54**, 258.

3 For examples of visible light induced C–O bond cleavage, see: (*a*) C. Dai, J. M. R. Narayanam and C. R. J. Stephenson, *Nat. Chem.*, 2011, **3**, 140; (*b*) G. L. Lackner, K. W. Quasdorf and L. E. Overman, *J. Am. Chem. Soc.*, 2013, **135**, 15342; (*c*) J. Jin and D. W. C. MacMillan, *Nature*, 2015, **525**, 87; (*d*) C. C. Nawrat, C. R. Jamison, Y. Slutskyy, D. W. C. MacMillan and L. E. Overman, *J. Am. Chem. Soc.*, 2015, **137**, 11270; (*e*) E. Speckmeier, C. Padie and K. Zeitler, *Org. Lett.*, 2015, **17**, 4818; (*f*) E. Speckmeier and K. Zeitler, *ACS Catal.*, 2017, **7**, 6821; (*g*) S.-F. Wang, X.-P. Cao and Y. Li, *Angew. Chem., Int. Ed.*, 2017, **56**, 13809; (*h*) E. Speckmeier, T. Fischer and K. Zeitler, *J. Am. Chem. Soc.*, 2018, **140**, 15353; (*i*) W. Xu, J. Ma, X.-A. Yuan, J. Dai, J. Xie and C. Zhu, *Angew. Chem., Int. Ed.*, 2018, **57**, 10357.

4 (*a*) J. D. Nguyen, B. S. Matsuura and C. R. J. Stephenson, *J. Am. Chem. Soc.*, 2014, **136**, 1218; (*b*) M. D. Kärkäs, I. Bosque, B. S. Matsuura and C. R. J. Stephenson, *Org. Lett.*, 2016, **18**, 5166; (*c*) I. Bosque, G. Magallanes, M. Rigoulet, M. D. Kärkäs and C. R. J. Stephenson, *ACS Cent. Sci.*, 2017, **3**, 621; (*d*) G. Magallanes, M. D. Kärkäs, I. Bosque, S. Lee, S. Maldonado and C. R. J. Stephenson, *ACS Catal.*, 2019, **9**, 2252.

5 J. Luo, X. Zhang, J. Lu and J. Zhang, *ACS Catal.*, 2017, **7**, 5062.

6 N. Luo, M. Wang, H. Li, J. Zhang, H. Liu and F. Wang, *ACS Catal.*, 2016, **6**, 7716.

7 For selected examples of intermolecular catalytic hydrogen transfer to biomass molecules, see: (*a*) H. Heeres, R. Handana, C. Dai, C. B. Rasrendra, B. Girisuta and H. J. Heeres, *Green Chem.*, 2009, **11**, 1247; (*b*) H. Kobayashi, H. Matsuhashi, T. Komanoya, K. Hara and A. Fukuoka, *Chem. Commun.*, 2011, **47**, 2366; (*c*) S. H. Mushrif, S. Caratzoulas and D. G. Vlachos, *Phys. Chem. Chem. Phys.*, 2012, **14**, 2637; (*d*) Q. Song, F. Wang, J. Cai, Y. Wang, J. Zhang, W. Yu and J. Xu, *Energy Environ. Sci.*, 2013, **6**, 994; (*e*) A. Shrotri, H. Kobayashi, A. Tanksale, A. Fukuoka and J. Beltramini, *ChemCatChem*, 2014, **6**, 1349.

8 (*a*) N. Luo, M. Wang, H. Li, J. Zhang, T. Hou, H. Chen, X. Zhang, J. Lu and F. Wang, *ACS Catal.*, 2017, **7**, 4571; (*b*) X. Wu, X. Fan, S. Xie, J. Lin, J. Cheng, Q. Zhang, L. Chen and Y. Wang, *Nat. Catal.*, 2018, **1**, 772.

9 S. Escoubet, G. Gastaldi, N. Vanthuyne, G. Gil, D. Siri and M. P. Bertrand, *J. Org. Chem.*, 2006, **71**, 7288.

10 (*a*) K. Qvortrup, D. A. Rankic and D. W. C. MacMillan, *J. Am. Chem. Soc.*, 2014, **136**, 626; (*b*) D. Hager and D. W. C. Macmillan, *J. Am. Chem. Soc.*, 2014, **136**, 16986; (*c*) J. D. Cuthbertson and D. W. C. MacMillan, *Nature*, 2015, **519**, 74.

11 Y.-R. Luo, *Handbook of Bond Dissociation Energies in Organic Compounds*, CRC Press, Boca Raton, 2003.

12 (*a*) J. L. Jeffrey, J. A. Terrett and D. W. C. MacMillan, *Science*, 2015, **349**, 1532; (*b*) I. C. Wan, M. D. Witte and A. J. Minnaard, *Chem. Commun.*, 2017, **53**, 4926.

13 I. Ghosh, L. Marzo, A. Das, R. Shaikh and B. König, *Acc. Chem. Res.*, 2016, **49**, 1566.

14 For a recent review of organic photocatalysts, see: N. A. Romero and D. A. Nicewicz, *Chem. Rev.*, 2016, **106**, 10075.

15 E. Speckmeier, T. G. Fischer and K. Zeitler, *J. Am. Chem. Soc.*, 2018, **140**, 15353.

16 Although the reductive potential of ketone intermediate **B** ($E_{\text{red}} < -1.7$ V *vs.* SCE) is more negative than that of 4CzIPN$^{\bullet -}$ ($E_{(\text{PC/PC}^{\bullet -})} = -1.24$ V *vs.* SCE), control experiment shows the ketone **B** can still be successfully reduced to afford the fragmentation products, see ESI†.